GEOTILL Inc.

Geotechnical Engineering • Subsurface Exploration • Environmental Services • Construction Testing and Material Engineering

GEOTECHNICAL ENGINEERING LIBRARY

GEOTILL

USA

GEOTILL

ENGINEERING, INC.

Phone 317-449-0033 Fax 317- 285-0609

info@geotill.com

Toll Free: 844-GEOTILL

Geotechnical, Environmental and Construction Materials Testing Professionals

www.geotill.com

Offices Covering all USA

Report of Seismic Piezocone Tests and Analysis Axial Pile Response at I-295 James River Bridge Richmond, Virginia

for
Federal Highway Administration
McLean, Virginia
FHWA DTFH61-98-00047

Submitted to:

SaLUT, Inc.
11609 Edmonston Road
Beltsville, MD 20705
Attn: Victor Elias

Field Testing Phase of Support Services TWR #35
SaLUT Project Number 98-190

Prepared by

Paul W. Mayne, PhD, P.E.
493 Guilford Circle
Marietta, GA 30068

June 2002

Report of Seismic Piezocone Tests and Analysis Axial Pile Response at I-295 James River Bridge Richmond, Virginia

for
Federal Highway Administration
McLean, Virginia
FHWA DTFH61-98-00047

Submitted to:

SaLUT, Inc.
11609 Edmonston Road
Beltsville, MD 20705
Attn: Victor Elias

Field Testing Phase of Support Services TWR #35
SaLUT Project Number 98-190

Prepared by

Paul W. Mayne, PhD, P.E.
493 Guilford Circle
Marietta, GA 30068

June 2002

June 20, 2002

Albert F. DiMillio
Geotechnical Team Leader
FHWA Turner-Fairbanks Laboratory
6300 Georgetown Pike, HRDI-8
McLean, VA 22101-2296

RE: ***Report of Seismic Piezocone Testing & Axial Pile Foundation Analysis***
I-295 James River Bridge, Richmond, Virginia
TWR #35; SaLUT Project Number 98-190
FHWA Contract DTFH61-98-00047

Dear Mr. DiMillio,

This report presents a description of the in-situ testing collection, derived seismic piezocone test (SCPTU) data, analytical procedures, and results of the load-displacement-capacity predictions for a driven concrete test pile foundation at the James River Bridge near Richmond, Virginia.

Executive Summary

The axial load-displacement-capacity response of pile foundations can be conveniently evaluated using the results of seismic piezocone penetration tests (SCPTU) to provide continuous profiles of small- and large-strain soil properties. The penetration readings (q_T, f_s, and u_b) reflect soil limit states that are utilized to obtain the axial side & base components for capacity calculations, while the initial soil-pile stiffness is assessed from measurements of downhole shear wave velocity (V_s) via elastic continuum theory. An equivalent elastic modulus coupled with degradation scheme provides nonlinear representation with increasing load level.

Cone penetration tests have been completed for this study, including seismic and resistivity type soundings. The data are processed and applied to a set of unpublished load tests on a driven PSC pile at the I-295 James River Bridge east of Richmond, Virginia. Results of the SCPTU are used to develop a nonlinear evaluation of the axial pile response and load transfer.

Introduction

The evaluation of deep foundations for support of bridges, walls, and buildings is usually separated into two analysis procedures: (1) capacity, and (2) displacements at working loads. In the calculations of capacity, different methods are available depending upon whether the loading is undrained or drained, the soils are fine-grained or granular or intermediate geomaterials, as well as the applied direction of loading (compression, uplift, lateral, or moment). Ultimate capacity calculations are formulated on the basis of static equilibrium, limit plasticity, wedge failure, and cavity expansion, as well as empiricism (Poulos & Davis, 1980). For

analyses involving displacements, methodologies are available based on spring coefficients or subgrade reaction (t-z curves, q-z curves, p-y curves), elastic continuum theory (E_s and ν), and empirical relationships. Details on the displacement approaches are succinctly summarized by Poulos (1989) and O'Neill and Reese (1999).

In reality, the axial response of deep foundations changes progressively from small strains that occur elastically at initial stress states (corresponding to the nondestructive region and K_0 conditions) and develop to elastic-plastic states corresponding to intermediate strains, eventually reaching plastic failure (as well as post-peak) conditions. Numerical approximations using finite elements, discrete elements, finite differences, and boundary elements can be used to follow the stress paths at points near and far from the soil-pile interfaces. However, simplified analytical methods also have merit in that quick and reliable assessments can be made using spreadsheets or programmable calculators.

With the recent popularity and advances in cone penetration testing for geotechnical site characterization, it is timely to discuss the use of seismic piezocone results for the evaluation of both capacity (obtained from the penetration data) and initial stiffness (E_0) for use in deformation response, especially since the test provides data at complete opposite ends of the stress-strain-strength response of soils. Since most foundations are constructed with more-than adequate factors of safety against full failure (FS > 3), the use of the initial stiffness for deformation assessment is truly more realistic, as conveyed by Figure 1 (Burns & Mayne, 1996). A modified hyperbola (Fahey & Carter, 1993) can be used to conveniently degrade the initial stiffness with increasing load level and provide nonlinear load-displacement-capacity results.

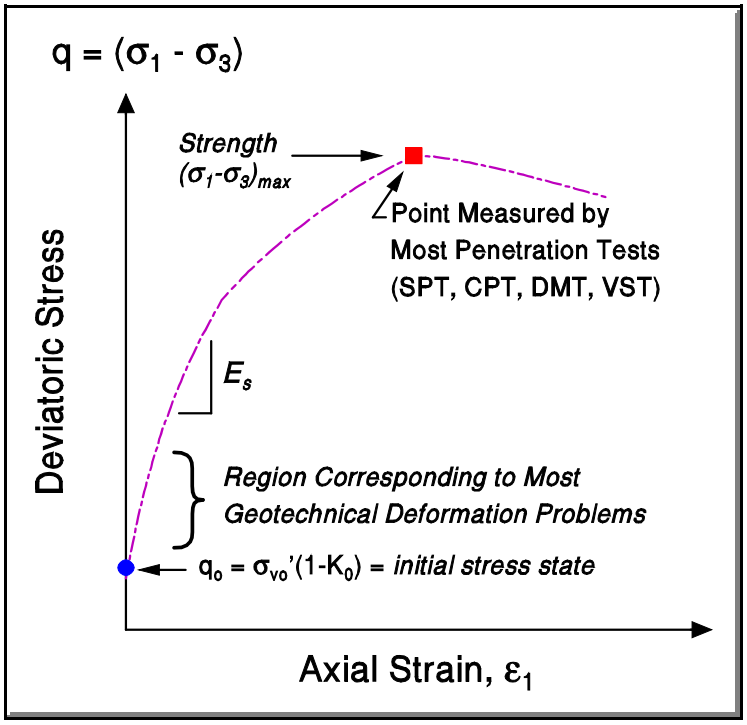

Figure 1. Associated Stresses and Stiffnesses at Small- and Large-Strains

Small-Strain Modulus

Recent research outside of the U.S. has found that the small-strain stiffness from shear wave velocity (V_s) measurements applies to the initial static monotonic loading, as well as the dynamic loading of geomaterials (Burland, 1989; Tatsuoka & Shibuya, 1992; LoPresti et al., 1993). Thus, the original dynamic shear modulus (G_{dyn}) has been re-termed the maximum shear modulus, designated G_{max} or G_0, that provides an upper limit stiffness given by: $G_0 = \rho_T V_s^2$ where ρ_T = total mass density of the soil. This is a fundamental stiffness of all solids in civil engineering and can be measured in all soil types from colloids, clays, silts, sands, gravels, to boulders and fractured rocks. The measurement is not hindered by the presence of groundwater, as in the case of P-wave measurements. The corresponding equivalent elastic modulus is found from: $E_0 = 2G_0 (1+\nu)$ where $\nu = 0.2$ is the value of Poisson's ratio of geomaterials at small strains.

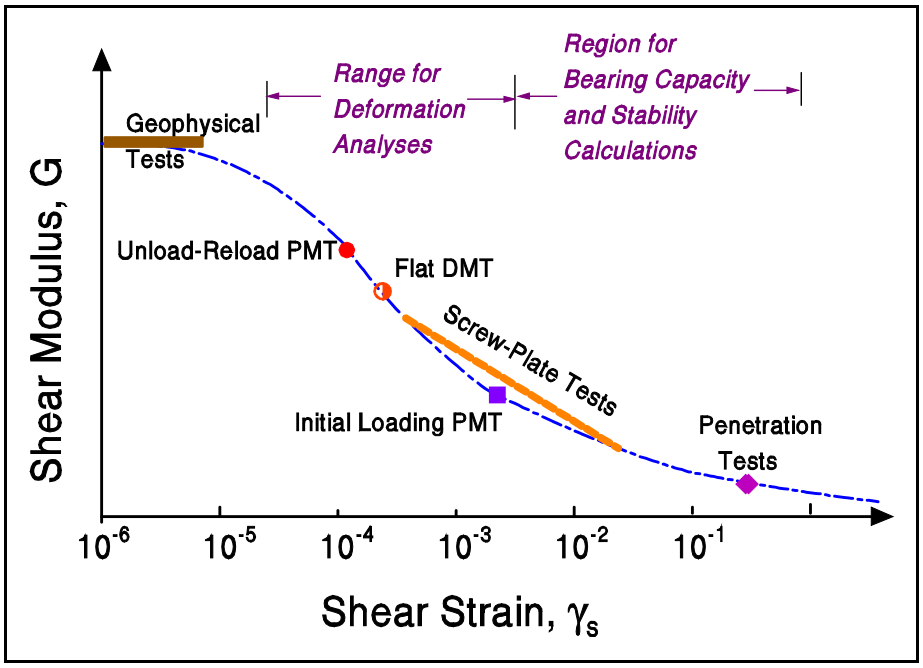

Figure 2. Variation of Shear Modulus with Strain Level and Relevance to In-Situ Tests.

The stress-strain-strength-time response of soils is complex, highly nonlinear, and depends upon loading direction, anisotropy, rate effects, stress level, strain history, time effects, and other factors. It is therefore a difficult issue to recommend a single test, or even a suite of tests, that directly obtains the relevant E_s for all possible types of analyses in every soil type. This is because the modulus varies considerably with strain level (or stress level). In certain geologic materials, it has in fact been possible to develop calibrated correlations between specific tests (e.g., PMT, DMT) with performance monitored data obtained from full-scale structures, including foundations and embankments, or with reference values from laboratory test. These tests will provide a modulus somewhere along the stress-strain-strength curve (Figure 2), yet not particularly well-defined with respect to its associated level of strain. Of particular note, the small-strain modulus from shear wave velocity measurements provides an excellent reference value, as this is the maximum stiffness that the soil can exhibit at a given void ratio and effective confining state. Herein, a generalized approach based on the small strain stiffness from shear wave measurements will be discussed, whereby the initial modulus (E_0) is degraded to an appropriate stress level for the desired factor of safety (FS).

The shear modulus degradation with shear strain is commonly shown in normalized form, with current G divided by the maximum G_{max} (or G_0). The relationship between G/G_0 and logarithm of shear strain is well recognized for dynamic loading conditions (e.g., Vucetic and Dobry, 1991), however, the monotonic static loading shows a more severe decay with strain, as seen in Figure 3. The monotonic curve has also been termed the "backbone curve". The cyclic curve is representative of data obtained from resonant column tests, whereas the monotonic curve has been recently addressed by special internal & local strain measurements in triaxial tests, as well as by torsional shear devices (Jamiolkowski, et al. 1994).

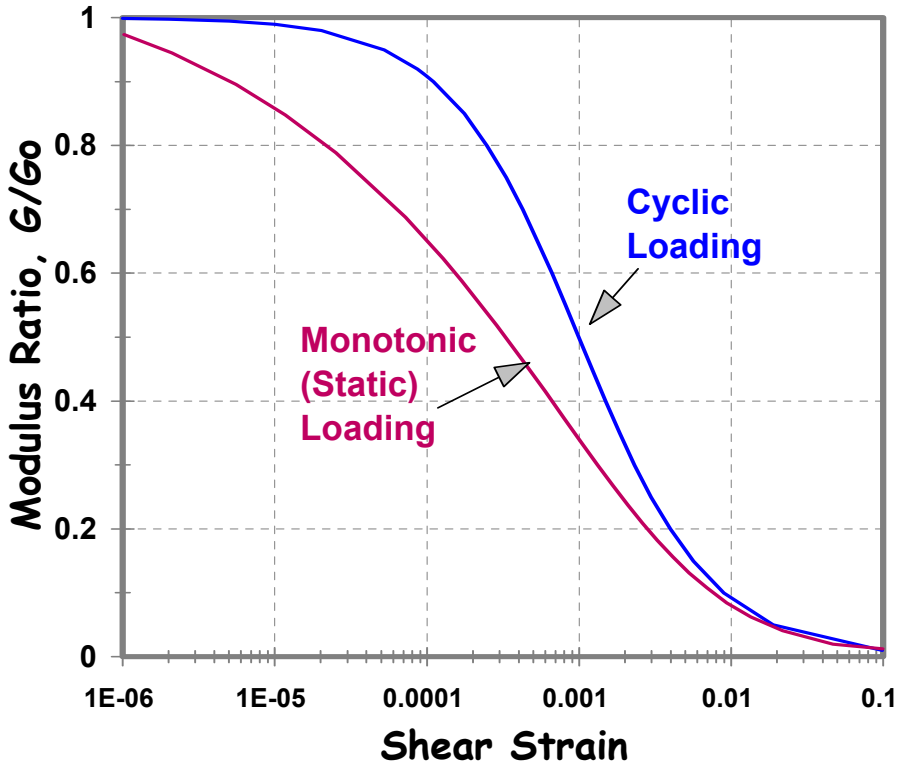

Figure 3. Modulus Degradation with Log Shear Strain for Initial Monotonic (Static) and Dynamic (Cyclic) Loading Conditions. Note: Strain as decimal.

In the past decade, major improvements in laboratory testing accuracy have been made in the U.K., Japan, and Italy. Laboratory monotonic shear tests with high-resolution deformation instrumentation have shown that strain data obtained external to the triaxial cells are flawed because of seating errors, bedding of the filter stone and paper, and boundary effects at the specimen ends. Thus, routine lab tests have shown soils to be softer than implied by field performance monitoring. New internal measurements are now possible that properly measure the soil stiffness at small- to intermediate-strains (LoPresti, et al. 1993, 1995; Tatsuoka & Shibuya, 1992). Figure 4 shows a comparison of the conventional external strain measurements and improved internal set of strain measurements taken on a triaxial test on North Sea Clay (Jardine, et al. 1984). The significant underevaluation of the stiffness using the common external displacement readings is apparent.

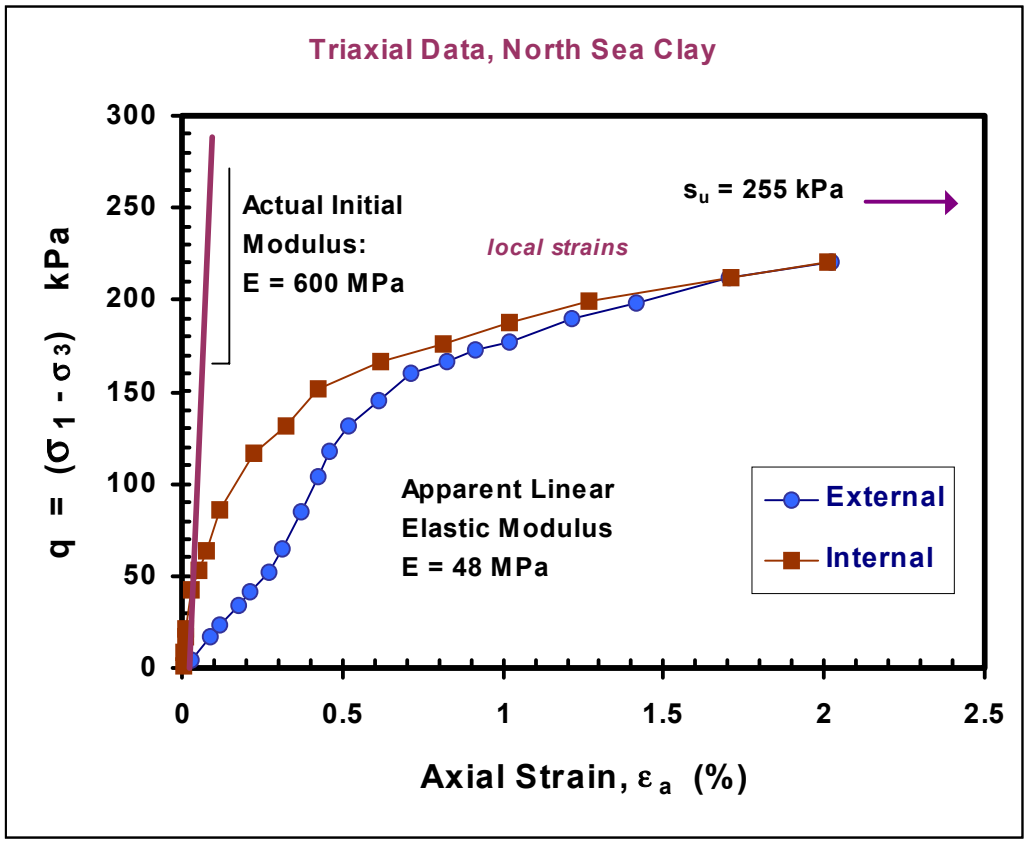

Figure 4. Improved Accuracy of Stiffness in Laboratory Testing Using Internal Local Strain Measurements Versus Conventional External Strains (data from Jardine, et al., 1984).

Many series of tests have now been completed using the internal local strain measurements. Different types of materials have been evaluated and the results are reported elsewhere (e.g., Yamashita, Jamiolkowski, and LoPresti, 2000). A selection of normalized moduli (E/E_{max}) with varying stress level (q/q_{ult}) obtained on uncemented, unstructured geomaterials is presented in Figure 5. Note here that an equivalent secant elastic modulus is used throughout. A modified hyperbola can be used as a simple means to reduce the small-strain stiffness (E_0) to secant values of E at working load levels, in terms of mobilized strength (q/q_{ult}). Figure 6 illustrates the suggested trends for unstructured clays and uncemented sands. The generalized form may be given as (Fahey & Carter, 1993):

$$E/E_{max} = 1 - f(q/q_{ult})^g \qquad (1)$$

where f and g are fitting parameters. Values of $f = 1$ and $g = 0.3$ appear reasonable first guestimates for unstructured and uncemented geomaterials (Mayne & Dumas, 1997; Mayne, et al. 1999a) and these provide a best fit for the data shown before in Figure 5. The mobilized stress level (q/q_{ult}) can also be considered as the reciprocal of the factor of safety (FS). That is, for $(q/q_{ult}) = 0.5$, the corresponding FS = 2.

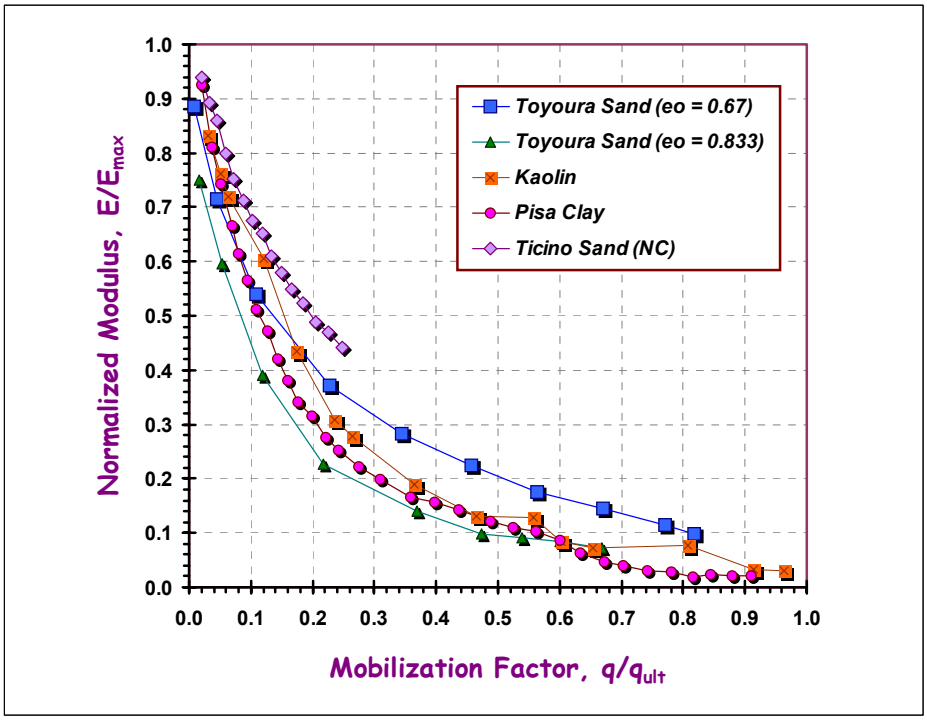

Figure 5. Modulus Degradation Response from Instrumented Laboratory Tests on Uncemented and Unstructured Geomaterials.

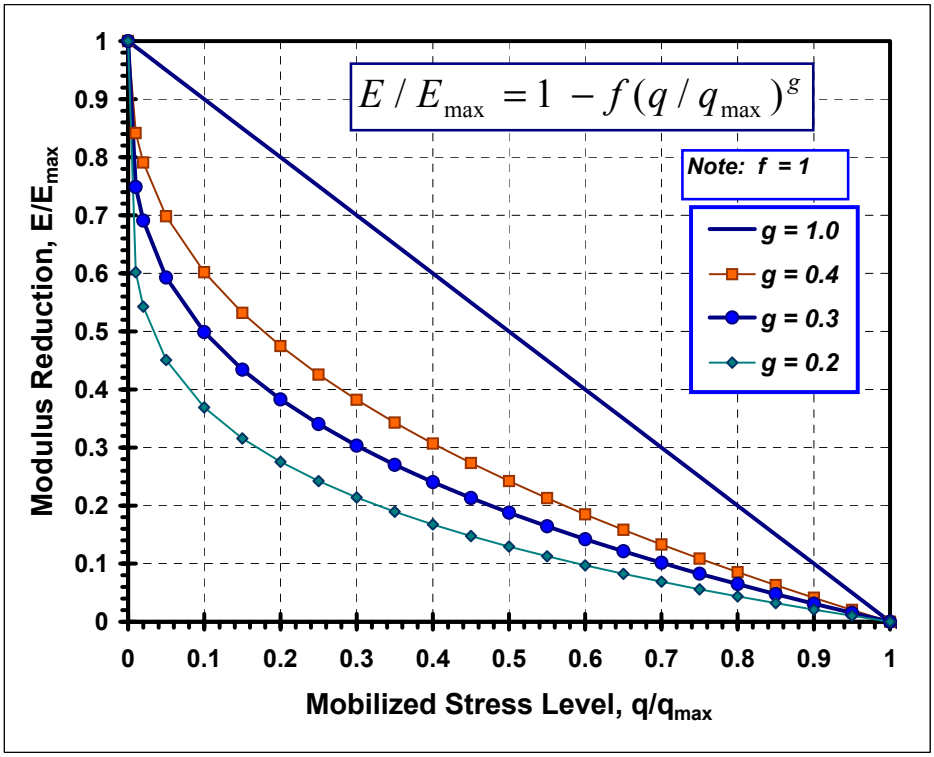

Figure 6. Modified Hyperbolas with g= 0.2, 0.3, and 0.4 for Modulus Degradation Curves. Note: Mobilized stress level q/q_u = 1/FS.

Other schemes for modulus degradation are available (e.g., Tatsuoka & Shibuya, 1992), several having a more fundamental basis and/or a better fitting over the full range of strains from small- to intermediate- to large-ranges (e.g., Puzrin & Burland, 1998). The intent here, however, is to adopt a simplified approach for facilitating the use of SCPTu data directly into foundation engineering analysis and for connecting small- and high-strain regions of soil response from shear wave and penetration data, respectively (Mayne & Dumas, 1997; Mayne, 1998).

Evaluating Axial Displacements

The axial load-displacement behavior of deep foundations may be represented by elastic continuum theory where solutions have been developed from boundary element formulations (Poulos & Davis, 1980), finite elements (Poulos, 1989), and approximate closed-form analytical solutions (Randolph & Wroth, 1978, 1979; Fleming et al. 1985). Continuum theory characterizes the soil stiffness by two elastic parameters: an equivalent elastic soil modulus (E_s) and Poisson's ratio (ν_s). Four generalized cases are considered: (1) homogeneous case where E_s is constant with depth; and (2) a Gibson-type condition where E_s is linearly-increasing with depth; (3) friction or floating-type piles; and (4) end-bearing type piles resting on a stiffer stratum. Figure 7 depicts the generalized stiffness profile for these cases, with corresponding definitions of moduli input for the analysis. The vertical displacement (w_t) of a pile foundation subjected to axial compression loading is expressed (Poulos, 1987, 1989):

$$w_t = P_t I_\rho / (E_{sL} d) \qquad (2)$$

P_t = applied axial load at the top of the pile foundation, E_{sL} = soil modulus along the sides at the full depth

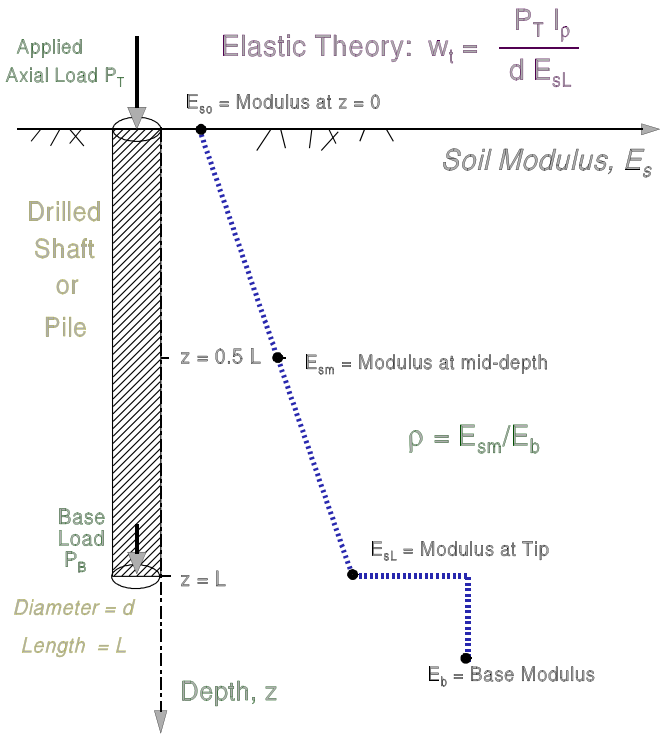

Figure 7. Soil Modulus Definitions and Terms Used in Elastic Continuum Model.

(z = L), d = foundation diameter, and I_ρ = influence factor. The factor I_ρ depends on the pile slenderness ratio (L/d), pile material, soil homogeneity, and relative soil-pile stiffness, as given in chart solutions, tables, or approximate closed-form. The latter is given in concise form (Randolph & Wroth, 1978, 1979; Poulos, 1987):

$$\mathbf{I_\rho} = 4(1+\nu) \frac{\left\{ 1 + \frac{1}{\pi\lambda} \frac{8}{(1-\nu_s)} \frac{\eta}{\xi} \frac{\tanh(\mu L)}{\mu L} \frac{L}{d} \right\}}{\left\{ \frac{4}{(1-\nu_s)} \frac{\eta}{\xi} + \frac{4\pi\rho}{\varsigma} \frac{\tanh(\mu L)}{\mu L} \frac{L}{d} \right\}} \tag{3}$$

where the following terms apply:

d = shaft diameter.
L = pile length.
η = d_b/d = eta factor (d_b = diameter of base, so that $\eta = 1$ for straight shafts).
ξ = E_{sL}/E_b = xi factor ($\xi = 1$ for floating pile; $\xi < 1$ for end-bearing).
ρ^* = E_{sm}/E_{sL} = rho ($\rho^* = 1$ for uniform soil; $\rho^* = 0.5$ for simple Gibson soil).
λ = $2(1+\nu_s)E_p/E_{sL}$ = lambda factor.
ς = $\ln\{[0.25 + (2.5\rho^*(1-\nu_s) - 0.25)\xi] (2L/d)\}$ = zeta factor.
μL = $2(2/\varsigma\lambda)^{0.5}$ (L/d) = mu factor.
E_p = pile modulus (concrete plus reinforcing steel).
E_{sL} = soil modulus value along pile shaft at level of base.
E_{sm} = soil modulus value at mid-depth of pile shaft.
E_b = soil modulus below foundation base (Note: $E_b = E_{sL}$ for floating pile).
ν_s = Poisson's ratio of soil.

Elastic continuum also provides an evaluation of axial load transfer distribution. The fraction of load transferred to the pile base (P_b) is given by (Fleming et al. 1985):

$$P_b/P_t = \frac{\left\{ \frac{4}{(1-\nu_s)} \frac{\eta}{\xi} \frac{1}{\cosh(\mu L)} \right\}}{\left\{ \frac{4}{(1-\nu_s)} \frac{\eta}{\xi} + \frac{4\pi\rho}{\varsigma} \frac{\tanh(\mu L)}{\mu L} \frac{L}{d} \right\}} \tag{4}$$

which conveniently has the same denominator as eq (3) for spreadsheet use. To account for the approximate nonlinear response, the modified hyperbola is used:

$$w_t = \frac{P_t \cdot I_\rho}{d \cdot E_{SL\max} \cdot [1-(P_t / P_{tULT})^{0.3}]} \tag{5}$$

Note that the displacement influence factor also depends on current reduced E_{sL}.so that I_ρ must be adjusted during incremental applied loading. The relative top displacement (w_t) to bottom deflection (w_b) is:

$$w_t/w_b = \cosh(\mu L) \tag{6}$$

Axial Capacity Determinations

The assessment of axial pile capacity ($Q_{ult} = Q_s + Q_b$) from CPT results is well-recognized (e.g., Robertson, et al. 1988; Poulos, 1989; Eslami & Fellenius, 1997). Of recent, Takesue, et al. (1998) offer a versatile direct CPT approach for side resistance of both drilled shafts and driven piles to obtain the pile side friction (f_p) in both clays and sands in terms of the measured f_s and excess porewater pressures (Δu_b) during piezocone penetration. Using measurements with a porous filter located at the cone shoulder:

$$\text{For } \Delta u_b < 300 \text{ kPa: then } f_p = f_s \cdot [(\Delta u_b/1250) + 0.76] \quad (7a)$$

$$\text{For } 300 \text{ kPa} < \Delta u_b < 1200 \text{ kPa: then } f_p = f_s \cdot [(\Delta u_b/200) - 0.50] \quad (7b)$$

In clays, the pile tip or pier base resistance (q_b) will be fully mobilized and can be evaluated from the effective cone resistance (Eslami & Fellenius, 1997):

$$\text{Clays: } q_b = q_t - u_b \quad (8)$$

In sands, however, full mobilization of the base develops fairly slowly, depending on the relative movement (s) with respect to pile width (B). Recent work by Lee & Salgado (1999) gives:

$$\text{Sands: } q_b \approx q_t \cdot [1.90 + \{0.62/(s/B)\}]^{-1} \quad (9)$$

AXIAL DRILLED SHAFT LOAD TEST, COWETA COUNTY, GEORGIA

The outlined procedure can be applied to a recent case study involving axial compression load testing of a drilled shaft for the widening and expansion of interstate I-85 in Coweta County, Georgia, south of Atlanta (Mayne & Schneider, 2001). The 0.91-m diameter shaft was constructed 19.2 m long under polymeric slurry to bear within the residuum and saprolite of the Piedmont geology. The base was situated in partially-weathered rock, as depicted in Figure 8. Results from standard penetration tests (SPT) in adjacent soil borings are also presented. The shaft was installed with an instrumented cage with 16 full-bridge electronic sister bars to measure load tranfer with depth during applied axial loads.

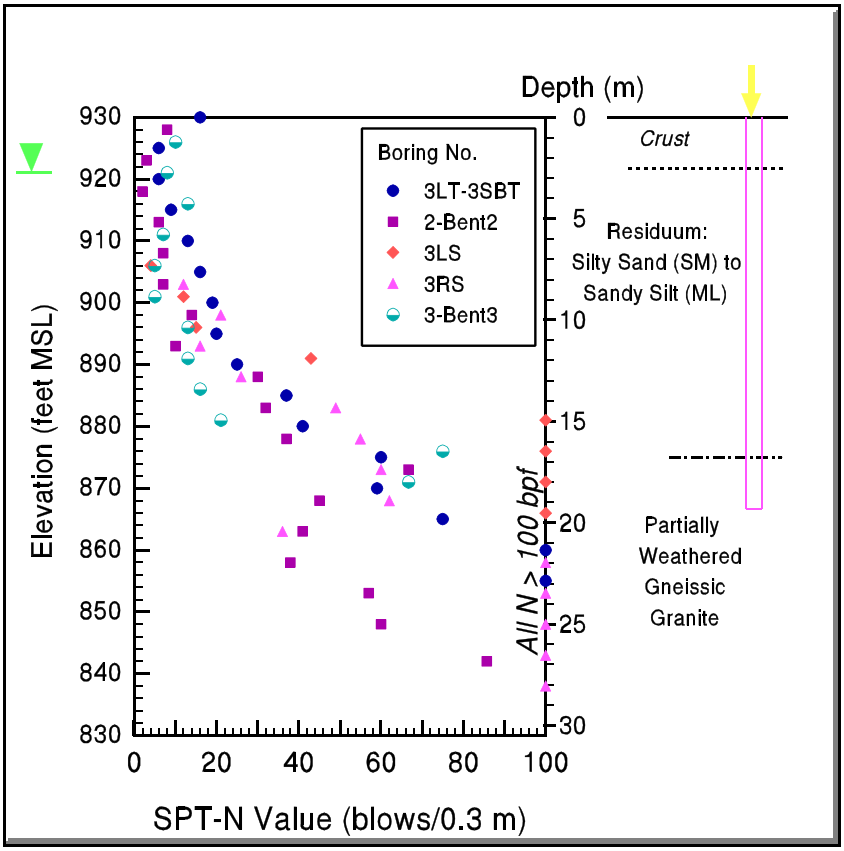

Figure 8. SPT Summary and Soil Profile, Coweta, GA.

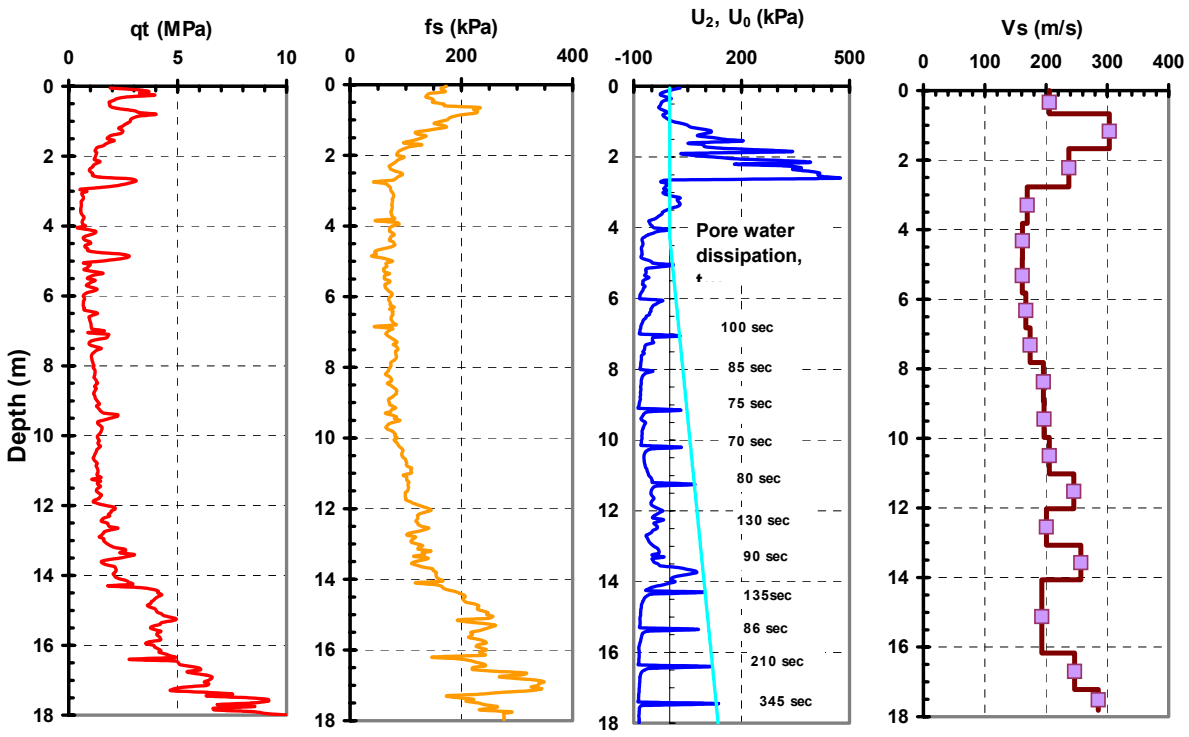

Figure 9. Results of Seismic Piezocone Sounding at Coweta Bridge Site.

In the Piedmont Geologic Province , the current overburden consists of residual soils that were derived from the in-place decomposition of the parent metamorphic and igneous rocks. These grade to saprolite and partially-weathered rock with depth (Sowers, 1994). Primary rock types include schist, gneiss, and granite, although localized regions include phyllite, slate, & diabase. The depth to parent rock varies locally because of differential weathering. Geotechnical categorization by the Unified Soils Classification System (USCS) place the residual materials as sandy silts (ML) and silty sands (SM), as discussed byMayne, et al. (2000).

Two piezocones soundings were conducted at the site using a 10-cm^2 Hogentogler penetrometer with very similar results. One of these was a seismic piezocone test with the four independent readings, as presented in Figure 9 (sounding B). Both the tip stress (q_t) and sleeve friction (f_s) show a crustal zone extending to about 3 meters depth, underlain by firm residual silts and sands, with harder saprolite encountered below depths of 15 meters. An interesting facet of the Piedmont is the continuous negative porewater pressures at the shoulder element (u_b or u_2) once the groundwater table is reached (Finke & Mayne, 1999). At the Coweta site, the water table is located 2.8 m deep. Generally, full dissipation occurred to hydrostatic within 1 to 3 minutes. The downhole measurement of shear wave velocity (V_s) confirmed presence of a 3-m crustal layer and the subsequent increase of stiffness with depth in the natural residuum.

A maximum tip stress of 32 MPa was recorded in the partially-weathered rock during sounding A. Assuming a maximum mobilized movement at the base of (s/B) = 10%, equation (9) gives a reduction factor (q_b/q_t) = 0.123, or unit base resistance of q_b = 3.95 MPa. For the base area A_b = 0.65 m^2, an end bearing component of Q_b = 2.56 MN is calculated. For each depth reading at 50-mm intervals, the unit side friction was calculated based on the Δu readings, giving an average f_p/f_s ratio = 0.71, and overall pile side resistance of f_p = 87 kPa per equation (7). For the total surface area of A_s = 55 m^2, the calculated total side capacity is Q_s = 4.78 MN. Thus, the total capacity of the shaft is evaluated as $Q_t = Q_s + Q_b$ = 7.24 MN from the CPT data. The shear wave data are processed to obtain the initial stiffness using a relationship for saturated soil mass density in terms of V_s and depth z (Mayne, et al., 1999a). The initial elastic modulus is found from:

$$E_{max} = 2\, G_{max}\, (1 + \nu) \qquad (10a)$$

$$G_{max} = \rho_t V_s^{\,2} \qquad (10b)$$

For the elastic continuum analysis of displacements, the initial soil modulus along the shaft at the full length (z = L) is taken as E_{sL} = 360 MPa, giving the modulus rho term $\rho^* = E_{sm}/E_{sL}$ = 0.5 for this site. The xi ratio is based on previous studies of end-bearing deep foundations in the Piedmont (Mayne, et al. 1999b) and taken as ξ = 0.25, or ratio E_{sL}/E_b = 4, although E_{sL}/E_b ratios of 1 to10 still provide reasonable predictions. A pile material modulus of E_p = 27.8 GPa is used for the drilled shaft.

The full predictions of total load, shaft load, and base load versus deflection at the top of the shaft are presented in Figure 10 in comparison with the measured axial loads and displacements. Also shown are the load transfer measurements to the base derived from the instrumented reinforcing cage. The nonlinear simulation is seen to well represent the nonlinear load-deflection response throughout the full testing range from 0 to 45 mm. In addition, the elastic continuum theory correctly proportions the amount of load distribution amongst the side and base components. For the final loading condition at 45 mm deflection, 72% of the total compression load is taken in side shear and 28% transfer to the base.

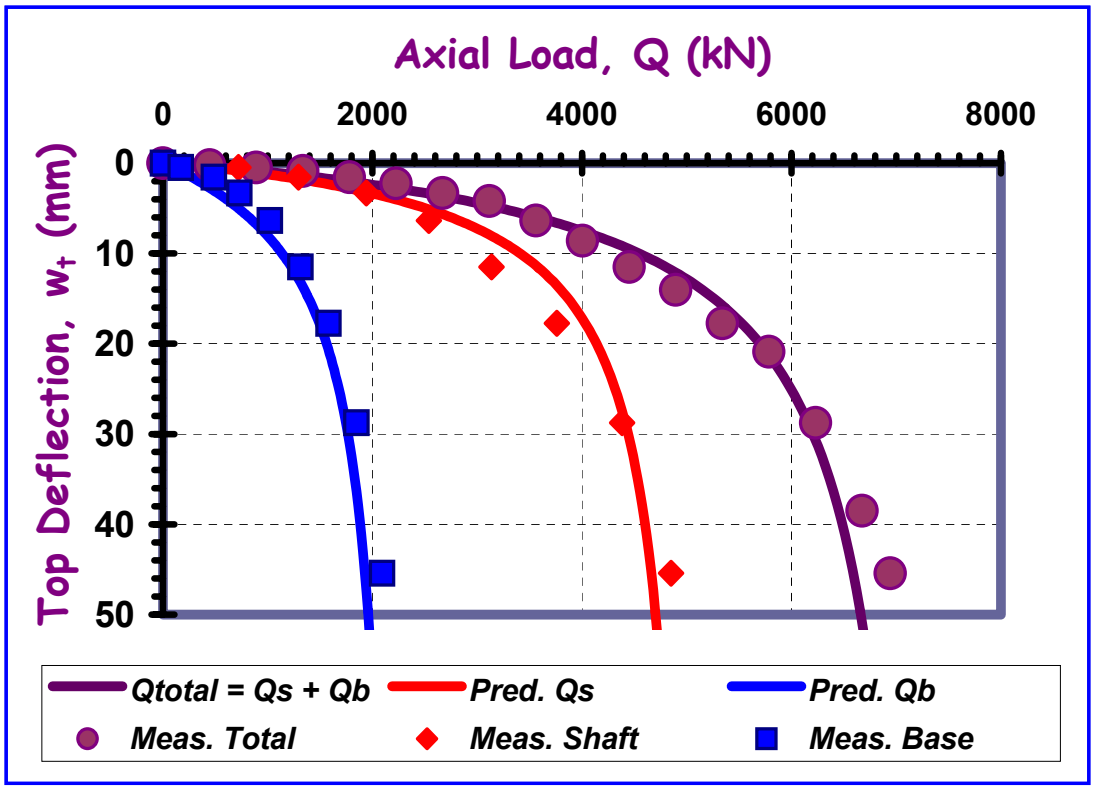

Figure 10. Measured and Predicted Axial Load-Displacement and Load Transfer Response of Drilled Shaft at I-85 Load Test, Coweta County, GA (Mayne & Schneider, 2001).

I-295 JAMES RIVER BRIDGE, RICHMOND, VIRGINIA

In the period from 1983 to 1988, the I-295 bridge over the James River was constructed east of Richmond, Virginia, in the counties of Henrico and Chesterfield. The project was designed by Figg & Muller as a cable-stayed concrete segmental bridge and has since been named the Enon-Varina Bridge. Twin parallel precast segments of 4680 feet long each were made for the north- & south-bound lanes (1425 m). The bridge was constructed by the joint venture of S.J. Groves and Peter Kiewit. The author at the time was a geotechnical consulting engineer with Law Engineering Associates of Virginia.

The two mainspan piers were designed for axial total loading of 40,000 kips each (178 MN). The foundations consisted of driven 24-inch (0.61-m) square prestressed concrete pilings of nominal ±50-foot lengths (±15-m). A total of 780 piles were installed for the project. Static axial load tests per ASTM D 1143 were conducted at 5 piles and additional pile driver analyzer tests were also performed to evaluate axial pile capacity. A design load of 250 tons (2225 kN) was selected by the VDOT.

Soil conditions consist of loose to firm alluvial sands, silts, and clays that overlie very dense sands & gravels of Pliocene to Pleistocene age. Occasional cobbles are found within the sediments. The general regions around the project are farmland. The north side of the river lies approximately 45 feet (+ 14 m) higher above the river elevation at +0 feet msl (+0 meters). A series of soil borings conducted by the VDOT included standard penetration tests (SPT) per ASTM D 1586. General locations of the borings on large spacings is shown in Figure 11.

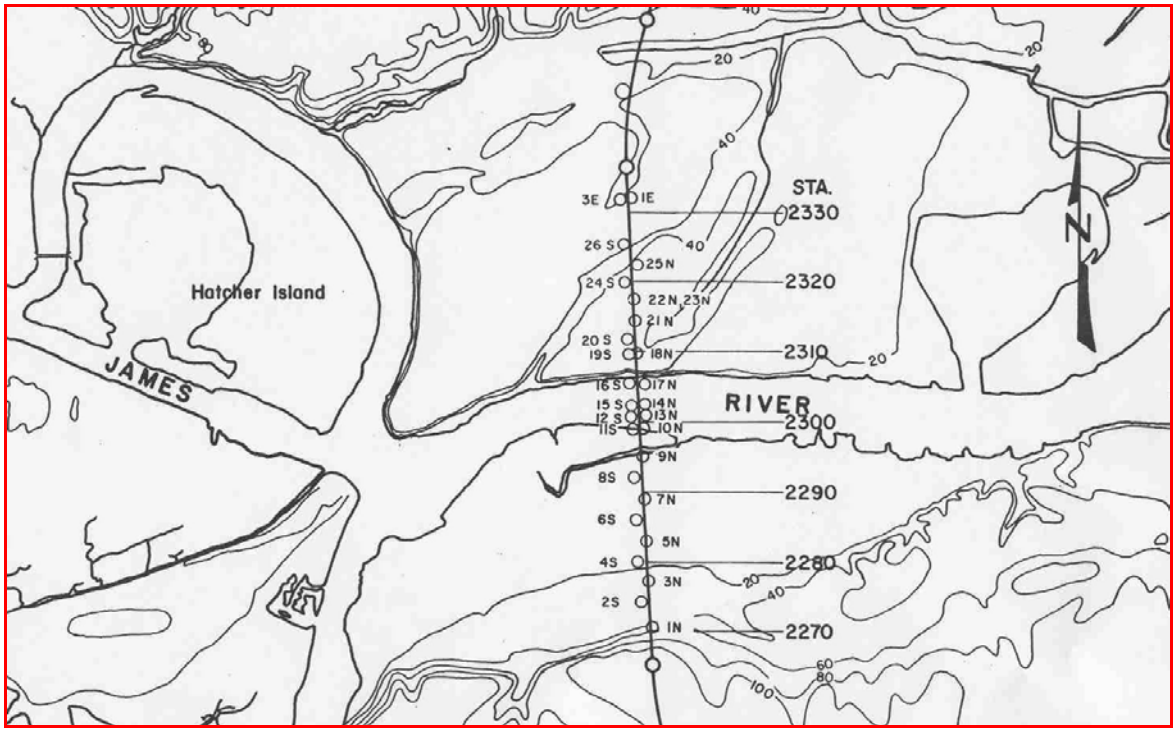

Figure 11. Soil boring locations along the I-295 James River Bridge alignment.
(Note: Stations are in feet).

In August 2000, the author revisited the site to collect additional in-situ test data at the site for comparison with CPT prediction methods. Only one test pile was accessible by the cone rig at this time due to property rights, access control, existing terrain, and utility conditions (Pier 23 south bound lane, SBL). This pile is located on the north side of the river and has an embedded length of 53 feet (16.2 m). Subsurface profiles for the north side of the bridge prepared from the boring records are presented in the appendix. A summary of the SPTs in the vicinity of Pier 23 SBL are shown in Figure 12. In general, the mean SPT N-value is about 15 bpf along the pile shaft.

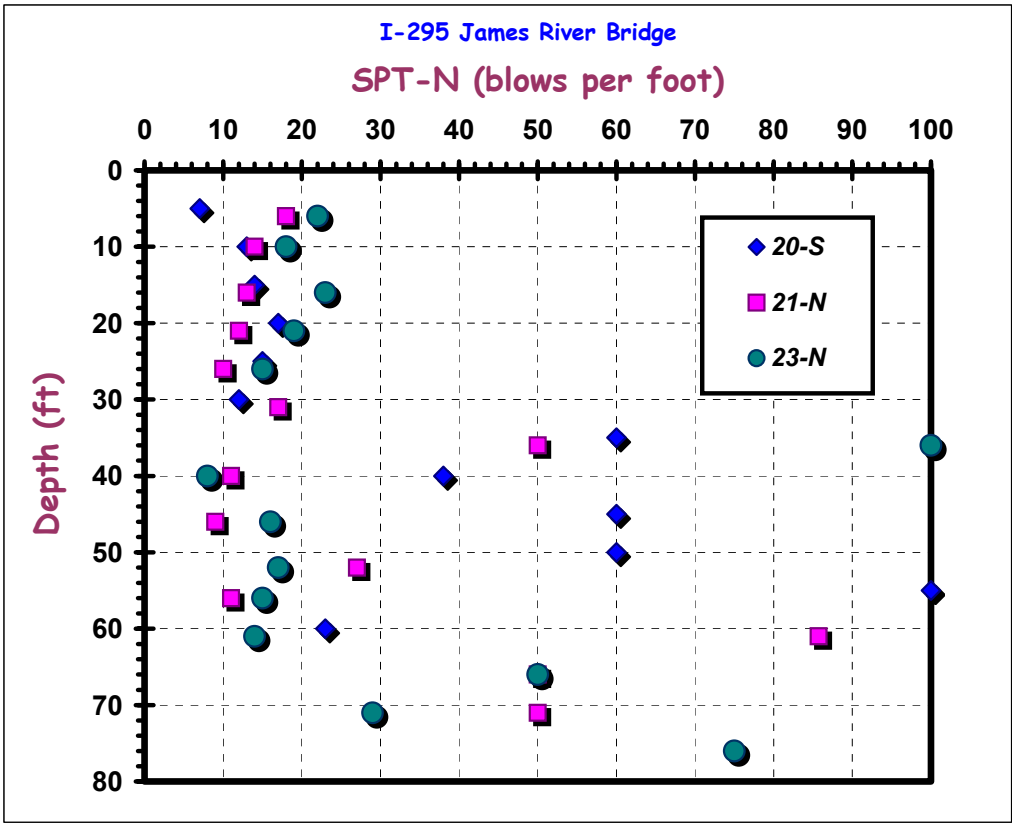

Figure 12. Summary of SPT N-values in vicinity of test pile pier 23 SBL at James River Bridge.

In the later testing, three cone penetration tests (CPT) were completed, however, they reached only 30-foot (10-m) depths because of a gravelly cobble layer. The layer is evident in the SPT results shown in Figure 12 above. The penetration portions of the CPTs were conducted according to ASTM D 5778 with continuous measurements of tip stress (q_t), sleeve friction (f_s), and porewater pressures (u_2) taken at the shoulder position. Inclination readings (i) of the verticality of the probe was also taken, but not reported. In two tests, downhole measurements of shear wave velocity were taken at approximate 3.3-foot (1-m) depth intervals using the procedures discussed by Campanella (1994). Figure 13 shows the results of the four channels of measurements from the two soundings. A third sounding was conducted using a resistivity module and the results are given in the appendix. Figure 14 shows the cone rig in operation at the bridge site. The rig uses twin earth anchors at the rear of the Ford 350 truck.

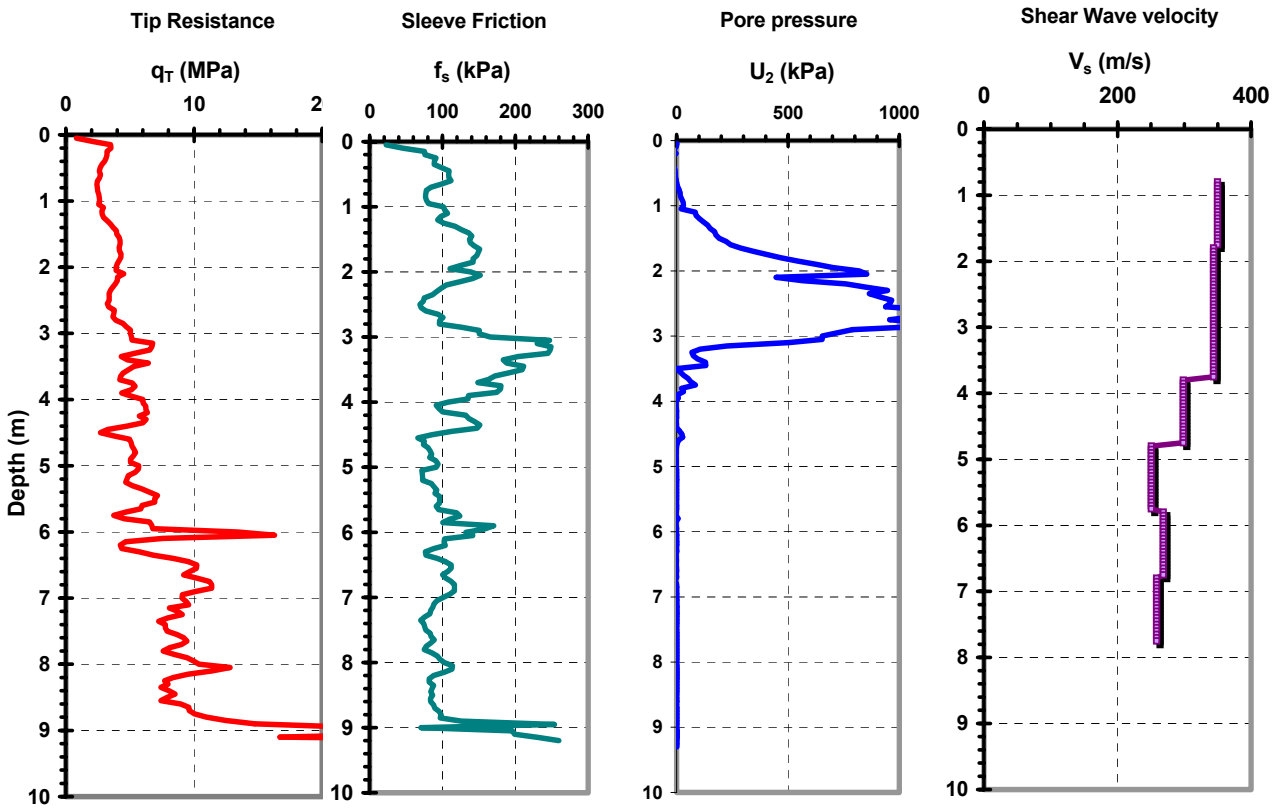

Figure 13. Results of seismic piezocone tests at I-295 James River Bridge site.

Figure 14. GT cone rig conducting CPTs near Pier 23 SBL at James River Bridge.

The load testing was conducted using a static load frame to hold the dead weight of available PSC pilings with a hydraulic jacking system to apply increments of axial loading to the piles. Loads were recorded using a calibrated load cell and checked with gage pressures from the hydraulic loading system. Deflections at the pile top were monitored using two dial gages, as well as a survey level and benchmark for backup readings. A telltale was installed at the tip (or toe) to measure the relative deflections and compression of the pile. One of the load test setups used at the site is shown in Figure 14. Results on Pier 23 SBL load test are presented in Figure 15.

Figure 14. Static load testing of PSC pile at main span Pier 17.

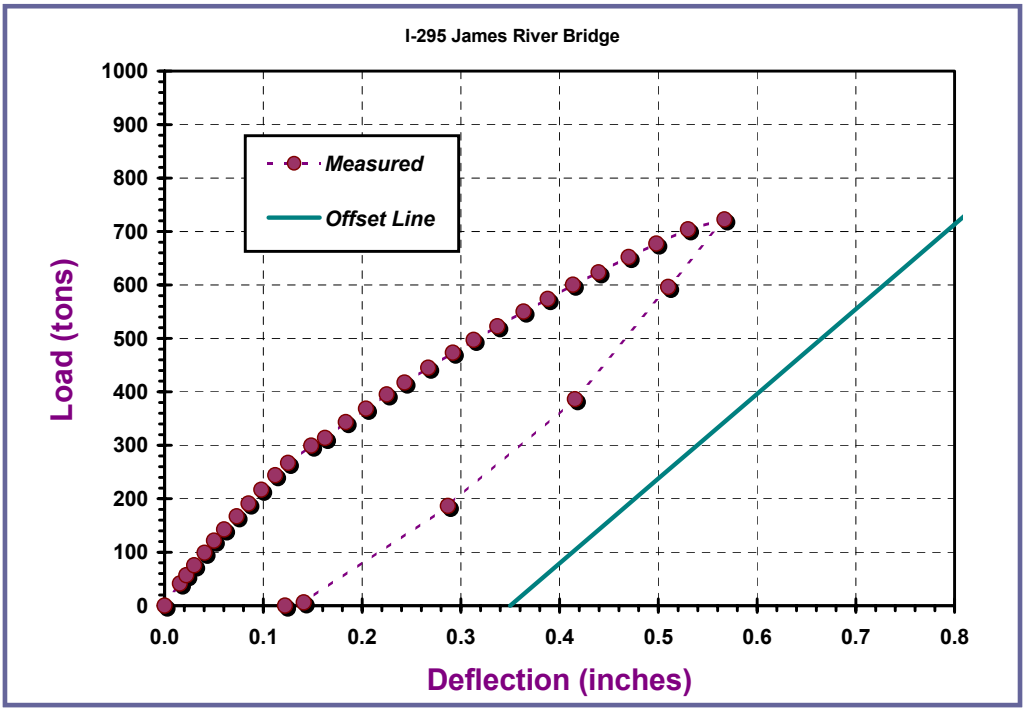

Figure 15. Axial load-displacement response for test pile at Pier 23 SBL

The axial capacity, as determined by the Davisson offset line criterion, is seen to be greater than the highest measured load applied to the pile. The calculation of capacity from the CPT data is difficult because the soundings penetrate only to 10 m because of the gravel & cobble layer. Nevertheless, using the results of sounding 02 at the site gives the following mean values of readings and parameters in Table 1 through the upper soil strata.. The direct side friction approach suggested by Takesue, et al. (1998) has been used in this case.

Table 1. Summary of Derived Values from Sounding SCPTu 02

Measurement or Parameter	***Mean Value or Calculated Value***
Cone tip stress, q_t	5.90 MPa
Measured sleeve friction, f_s	111 kPa
Penetration porewater pressure, u_2	146 kPa (Also, Δu_2)
Ratio pile friction to cone friction, f_p/f_s	1.21
Evaluated pile side friction, f_p	135.4 kPa
Pile side surface area, $A_s = 4\ d\ L$	39.4 m^2
Estimated end bearing, q_b	5900 kPa
Pile end area, $A_b = B^2$	0.372 m^2
Shaft capacity, $P_s = f_p A_s$	5332 kN
Tip capacity, $P_b = q_b A_b$	2193 kN
Total Capacity, $P_t = P_s + P_b$	7525 kN

From the shear wave data, the mean value of initial elastic modulus from sounding SCPTU 02 is 425 MPa and an assumed ratio of base to side stiffness is 4 (see Coweta results). This can be input into the aforementioned elastic continuum model with the modified hyperbola used to reduce the modulus as the load levels are increased (and associated FOS decreases). Figure 16 shows the comparison of measured and predicted nonlinear load-displacement response for the PSC pile at Pier 23 SBL. Considering the fact that end bearing elevations were not reached by the CPT, the comparison is quite good. The measured and estimated response of the telltales at the tip are given in Figure 17. Fair agreement is evident, yet the general trend is seen to be reasonable.

Conclusions

Results of seismic piezocone tests can be useful in providing data for both capacity calculations and small-strain stiffness from a single sounding. The shear wave provides a fundamental initial stiffness for the evaluation of foundation systems and a modulus degradation scheme is used to approximate nonlinear effects.. An elastic continuum formulation can be used to represent the axial load-displacement response and proportion of load transfer in side and base resistance. The method was applied to SCPTU data obtained at the I-295 James River Bridge site in comparison with axial load tests on a driven concrete piling.

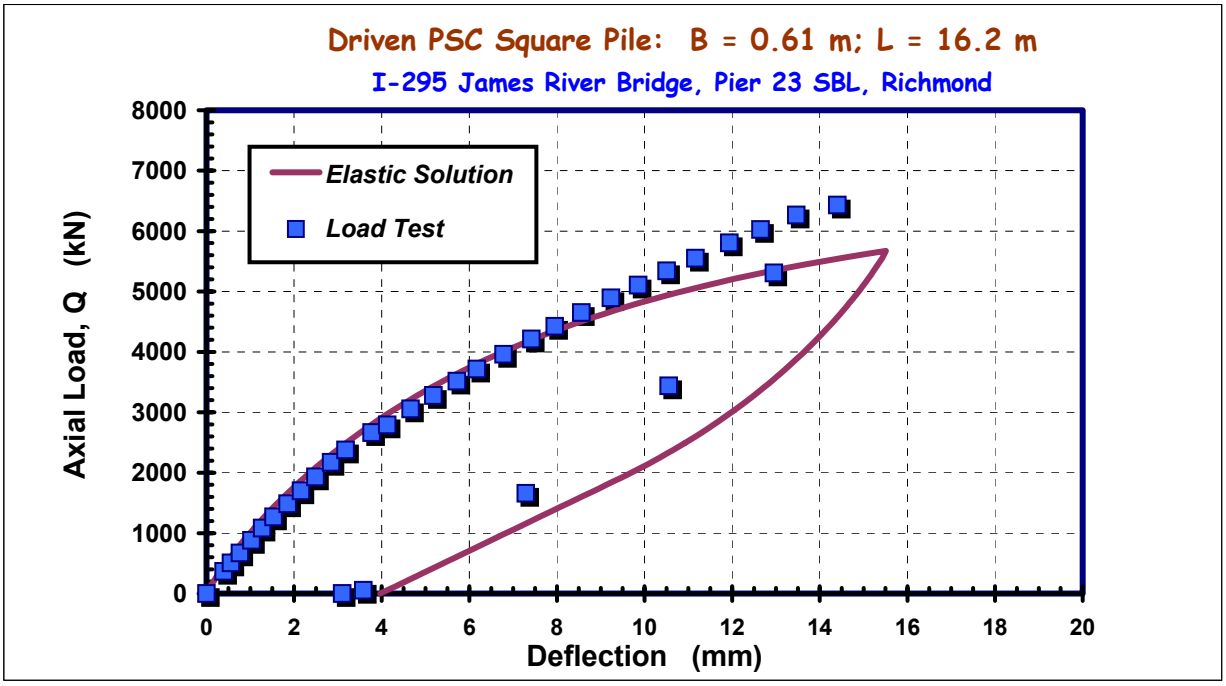

Figure 16. Measured and predicted axial load response of prestressed concrete pile at James River.

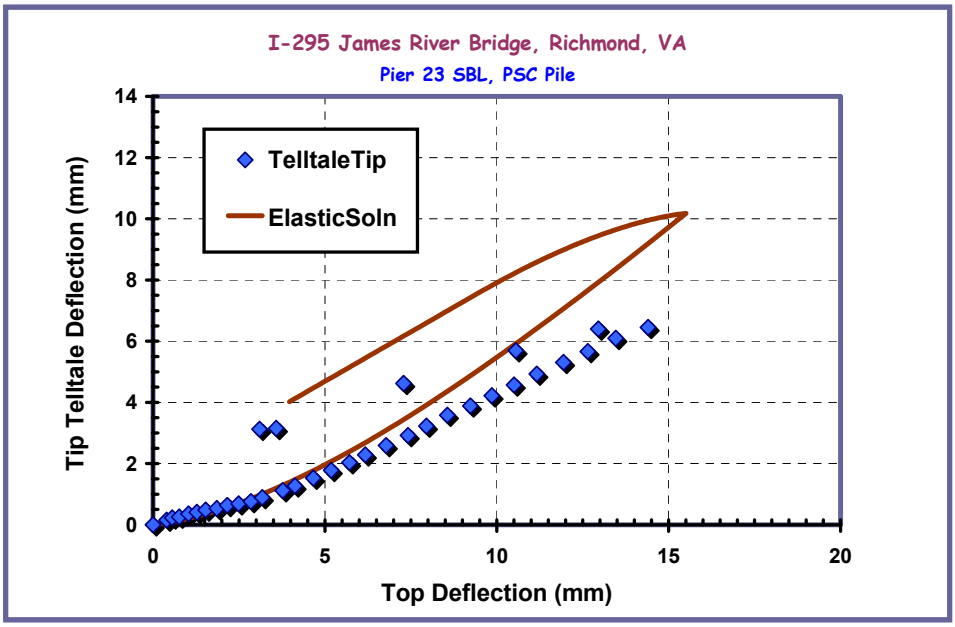

Figure 17. Measured and predicted telltale response of concrete pile at James River.

Figure 18. Views of the I-295 Bridge over the James River, Richmond, Virginia.

Should you have any questions or comments regarding these results, please contact the undersigned.

Sincerely,

Paul W. Mayne, PhD, P.E.

Office: 404-894-6226
Fax: 404-894-2281
Email at GT: pmayne@ce.gatech.edu

Acknowledgments

Thanks to Tom Pelnik, Don Akers, and Bob Riley of the Virginia DOT for providing access and clearance to the James River Bridge Site. Appreciation is extended to Tom Scruggs of the Georgia DOT in gaining site access at the Coweta County, GA site and to Professor Mike O'Neill of the University of Houston in conducting and providing the results of that load test.

References

Burland, J.B. (1989). Small is beautiful: The stiffness of soils at small strains. *Canadian Geotechnical Journal* 26 (4), 499-516.

Burns, S.E. and Mayne, P.W. (1996). Small- and high-strain soil properties using the seismic piezocone. *Transportation Research Record* 1548, National Academy Press, Washington, D.C., 81-88.

Campanella, R.G. (1994). Field methods for dynamic geotechnical testing. *Dynamic Geotechnical Testing II*, STP 1213, ASTM, West Conshohocken, PA, 3-23.

Eslami, A. and Fellenius, B.H. (1997). Pile capacity by direct CPT and CPTu methods applied to 102 cas histories. *Canadian Geotechnical Journal* 34 (6), 886-904.

Fahey, M. and Carter, J. (1993). A finite element study of the pressuremeter using a nonlinear elastic plastic model. *Canadian Geotechnical Journal* 30 (2), 348-362.

Finke, K.A., Mayne, P.W. and Klopp, R.A. (1999). Characteristic piezocone response in Piedmont residual soils. *Behavioral Characteristics of Residual Soils*. GSP No. 92, ASCE, Reston/VA, 1-11.

Fleming, W.G.K., Weltman, A.J., Randolph, M.F., and Elson, W.K. (1985). *Piling Engineering*, Surrey University Press, Wiley & Sons, New York, 380 p.

Jamiolkowski, M., Lancellotta, R., LoPresti, D.C.F. and Pallara. O. (1994). Stiffness of Toyoura sand at small and intermediate strain, *Proc. 13th Intl. Conf. on Soil Mechanics & Foundation Engineering* (3), New Delhi, 169-173.

Jardine, R.J., Symes, M.J., and Burland, J.B. (1984). The measurement of stiffness in the triaxial apparatus. *Geotechnique* 34 (3), 323-340.

Lee, J.H. and Salgado, R. (1999). Determination of pile base resistance in sands. *Journal of Geotechnical & Geoenvironmental Engineering* 125 (8), 673-683.

LoPresti, D.C.F., Pallara, O., Lancellotta, R., Armandi, M., and Maniscalco, R. (1993). Monotonic and cyclic loading behavior of two sands at small strains, ASTM *Geotechnical Testing Journal* 16 (4), 409-424.

LoPresti, D.C.F., Pallara, O. and Puci, I. (1995). A modified commercial triaxial testing system for small-strain measurements. ASTM *Geotechnical Testing Journal* 18 (1), 15-31.

Mayne, P.W. (2000). Geotechnical site characterization by seismic piezocone tests. *Proceedings, the Fourth International Geotechnical Engineering Conference*, Cairo University, Egypt, 91-120.

Mayne, P.W., Brown, D.A., Vinson, J., Schneider, J.A. and Finke, K.A. (2000). Site characterization of Piedmont residual soils at the NGES, Opelika, AL. *National Geotechnical Experimentation Sites*, GSP No. 93, ASCE, Reston, VA, 160-185.

Mayne, P.W, and Dumas, C. (1997). Enhanced in-situ geotechnical testing for bridge foundation analyses. *Transportation Research Record 1569*, National Academy Press, Washington, D.C., 26-35.

Mayne, P.W. and Elhakim, A. (2002). Axial pile response evaluation by geophysical piezocone tests. Proceedings, 9th International Conference on Piling & Deep Foundations, Nice, France, Deep Foundations Institute.

Mayne, P.W., Martin, G.K., and Schneider, J.A. (1999b). Flat dilatometer modulus applied to drilled shafts in the Piedmont residuum. *Behavioral Characteristics of Residual Soils*. GSP No. 92, ASCE, Reston/VA, 101-112.

Mayne, P.W., Schneider, J.A., and Martin, G.K. (1999a). Small- and large-strain soil properties from seismic flat plate dilatometer tests. *Pre-Failure Deformation Characteristics of Geomaterials*, Vol. 1, (Torino), Balkema, Rotterdam, 419-426.

Mayne, P.W. and Schneider, J.A. (2001). Evaluating axial drilled shaft response by seismic cone. *Foundations & Ground Improvement,* GSP 113, ASCE, Reston/VA, 655-669.

Mayne, P.W. and Swanson, P.G. (1984). Geotechnical report: Final phase: I-295 James River Bridge. Law Engineering Report W3-3836; F&M Report 195-03; McLean, VA; 60 p.

O'Neill, M.W. and Reese, L.C. (1999). *Drilled Shafts: Construction Procedures & Design Methods*, Volumes I & II, Publication No. FHWA-IF-99-025, U.S. Dept. of Transportation, published by ADSC, Dallas, 758 p.

Poulos, H.G. and Davis, E.H. (1980), *Pile Foundation Analysis and Design*, Wiley & Sons, New York, 397 p. (reprinted by Krieger Publishing, Florida, 1990).

Poulos, H.G. (1987). From theory to practice in pile design (E.H. Davis Memorial Lecture). *Transactions*, Australian Geomechanics Society, Sydney, 1-31.

Poulos, H.G. (1989). Pile behavior: theory and application", 29th Rankine Lecture, *Geotechnique*, Vol. 39, No. 3, September, 363-416.

Puzrin, A.M. and Burland, J.B. (1998). Nonlinear model of small-strain behavior of soils. *Geotechnique* 46 (1), 157-164.

Randolph, M.F. and Wroth, C.P. (1978). Analysis of deformation of vertically loaded piles. *Journal of the Geotechnical Engineering Division*, ASCE, Vol. 104 (GT12), 1465-1488.

Randolph, M.F. and Wroth, C.P. (1979). A simple approach to pile design and the evaluation of pile tests. *Behavior of Deep Foundations*, STP 670, ASTM, 484-499.

Robertson, P.K., Campanella, R.G., Davies, M.P. and Sy, A. (1988). Axial capacity of driven piles in deltaic soils using CPT. Penetration Testing 1988 (2), Balkema, Rotterdam, 919-928.

Sowers, G.F. (1994). Residual soil settlement related to the weathering profile. *Vertical and Horizontal Deformations of Foundations & Embankments*, Vol. 2, (GSP No. 40), ASCE, New York, 1689-1702.

Takesue, K., Sasao, H., and Matsumoto, T. (1998). Correlation between ultimate pile skin friction and CPT data. *Geotechnical Site Characterization* (2), Balkema, Rotterdam, 1177-1182.

Tatsuoka, F. and Shibuya, S. (1992). Deformation characteristics of soils and rocks from field and laboratory tests. *Report of the Institute of Industrial Science*, Vol. 37, No. 1, Serial No. 235, The University of Tokyo, 136 p.

Vucetic, M. and Dobry, R. (1991). Effect of soil plasticity on cyclic response. *Journal of Geotechnical Engineering* 117 (1), 89-107.

Yamashita, S., Jamiolkowksi, M., and LoPresti, D.C.F. (2000). Stiffness nonlinearity of three sands. ASCE *Journal of Geotechnical & Geoenvironmental Engineering* 126 (10), 929-938.

Appendix

Seismic Piezocone Tests and SPT Data
Axial Pile Response at I-295 James River Bridge
Richmond, Virginia

for
Federal Highway Administration
McLean, Virginia
FHWA DTFH61-98-00047

Submitted to:

SaLUT, Inc.
11609 Edmonston Road
Beltsville, MD 20705
Attn: Victor Elias

Field Testing Phase of Support Services TWR #35
SaLUT Project Number 98-190

June 2002

Subsurface Profiles at North Side of James River Bridge

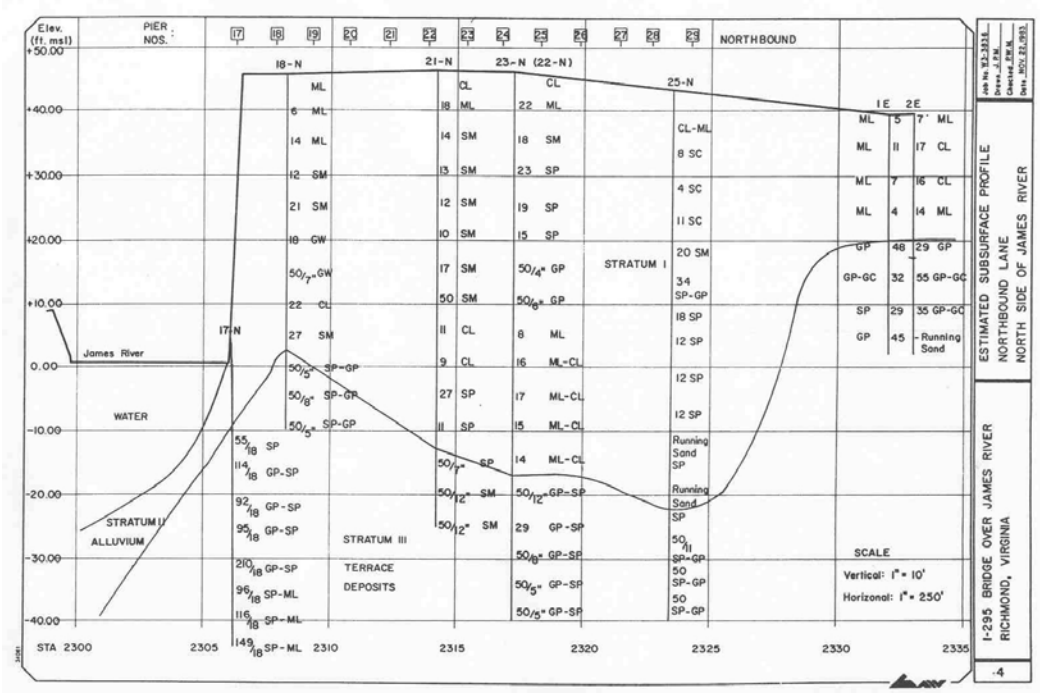

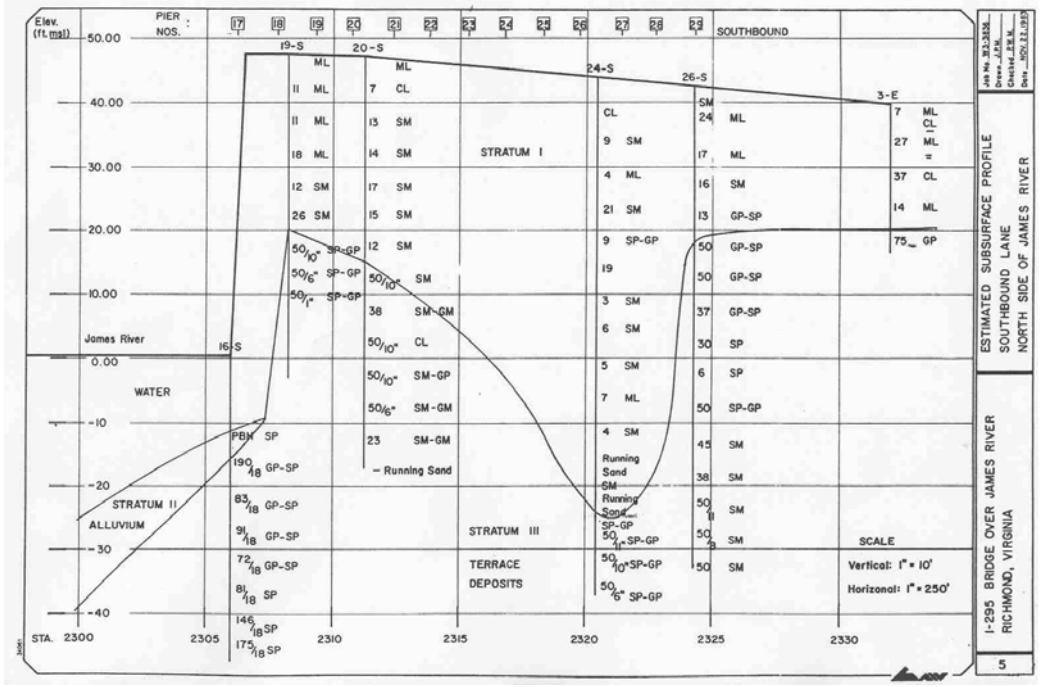

SCPTU 01 at James River Bridge

Seismic Piezocone Penetration Test — **Civil and Environmental Engineering**

In-Situ Research Division/Geosystems — **Georgia Institute of Technology**

Test Site: Varina Enon Bridge	File name: RICH01	Truck: GT Geostar	Date: 25-Jul-00
Location: Richmond, VA	Sounding: RICH01	Cone Hogentogler 10-tonne	Supervisor: Alec McGillivray
Client: FHWA	Latitude: N 37.38298	Area: 10 cm²	Operator: Guillermo Zavala
Project: VA DOT	Longitude: W 77.34672	Filter: Type 2	Inspector: Tianfei Liao
James River Bridge I-295	GWT: N/A	ASTM: D 5778	Review: Paul Mayne

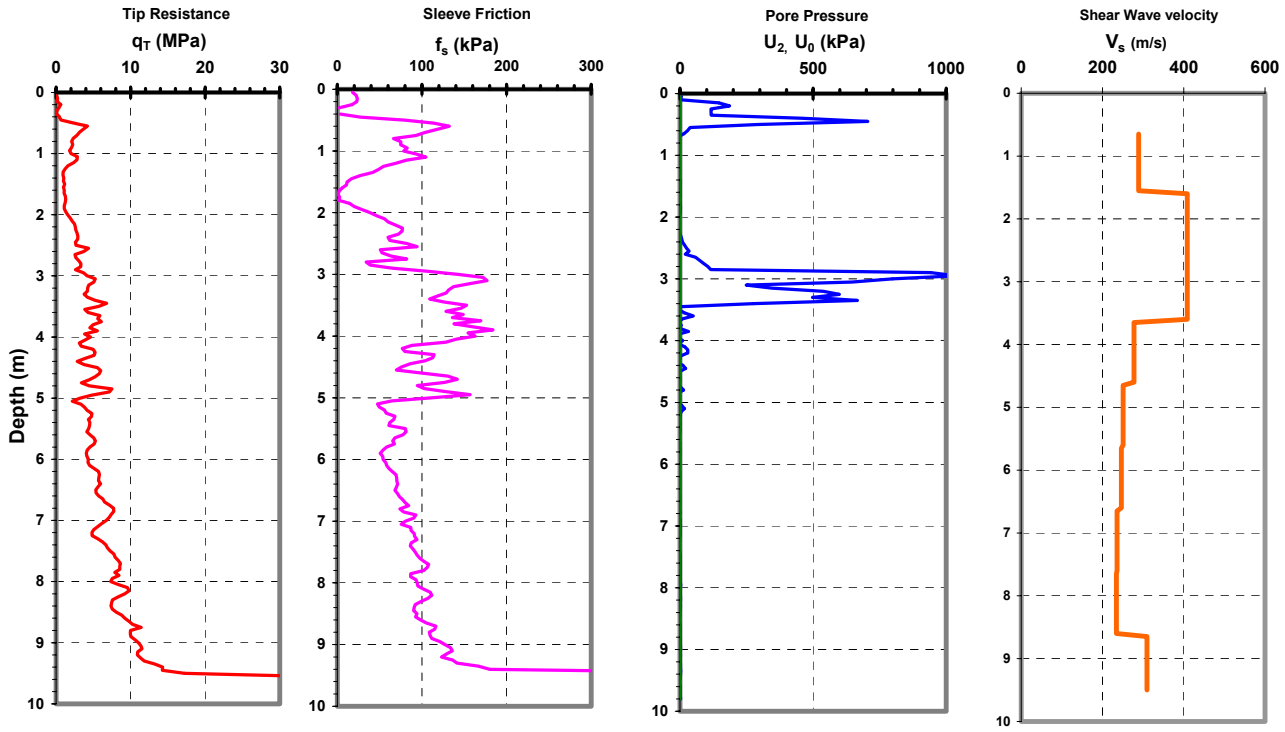

SCPTU 02 at James River Bridge

Seismic Piezocone Penetration Test — **Civil and Environmental Engineering**

In-Situ Research Division/Geosystems — **Georgia Institute of Technology**

Test Site: Varina Enon Bridge	File name: RICH02	Truck: GT Geostar	Date: 26-Jul-00
Location: Richmond, VA	Sounding: RICH02	Cone Hogentogler 10-tonne	Supervisor: Alec McGillivray
Client: FHWA	Latitude: N 37.38320	Area: 10 cm²	Operator: Guillermo Zavala
Project: VA DOT	Longitude: W 77.34664	Filter: Type 2	Inspector: Tianfei Liao
I-295 James River Bridge	GWT: N/A	ASTM: D 5778	Review: Paul Mayne

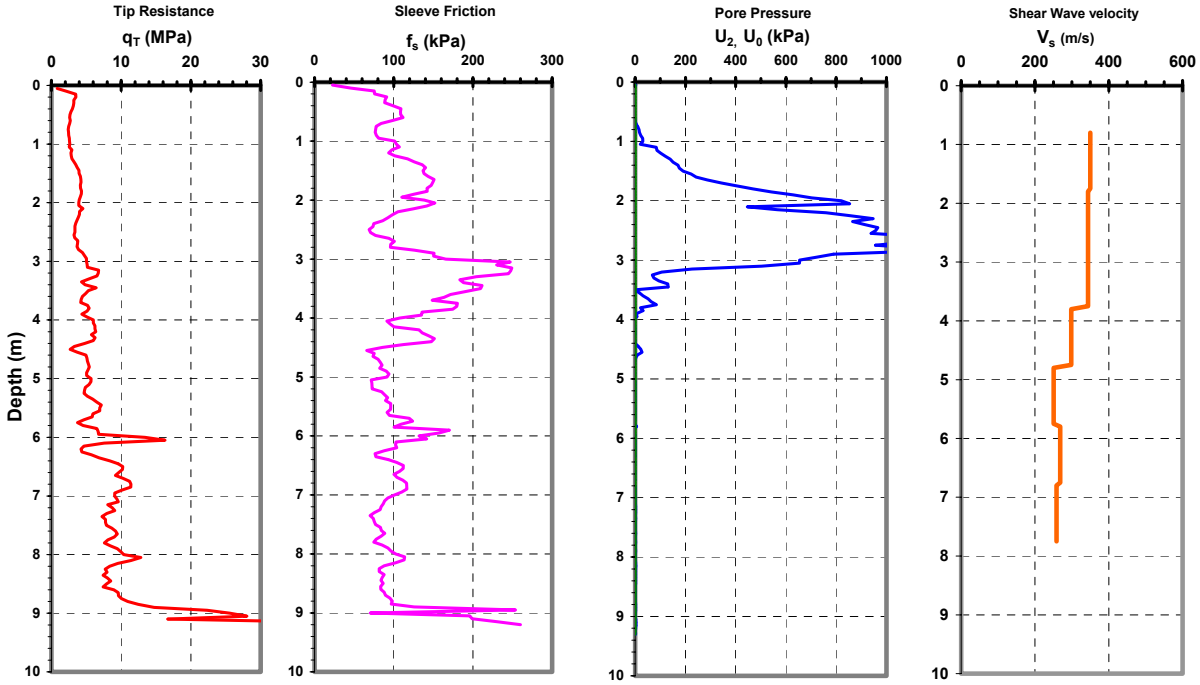

Type 1 CPTU at I-295 James River Bridge

Seismic Piezocone Penetration Test — Civil and Environmental Engineering

In-Situ Research Division/Geosystems — Georgia Institute of Technology

Test Site:	Varina Enon Bridge	File name:	RICH03	Truck:	GT Geostar	Date:	26-Jul-00
Location:	Richmond, VA	Sounding:	RICH03	Cone	Hogentogler 10-tonne	Supervisor:	Alec McGillivray
Client:	FWHA	Latitude:	N 37.38320	Area:	10 cm²	Operator:	Guillermo Zavala
Project:	TWR #35 (Salut)	Longitude:	W 77.34664	Filter:	Type 1	Coordinator:	Tianfei Liao
Contact:	Tom Pelnik (VA DOT)	GWT:	N/A	ASTM:	D 5778	Review:	Paul Mayne